An Efficient WOLA Structured OQAM-FBMC Transceiver

Jae Hoon Park
School of electronic engineering
Soongsil University
Seoul, Korea
pjh901118@ssu.ac.kr

Won Choel Lee
School of electronic engineering
Soongsil University
Seoul, Korea
wlee@ssu.ac.kr

***Abstract*— In this paper, we evaluate and analyze performance of these systems with windowed overlap-add (WOLA) technique. The offset quadrature amplitude modulation - filter bank basis multi carrier (OQAM-FBMC) has been attracted. OQAM-FBMC was nominated as one of new waveforms for 5G communications due to its capability of frequency selectivity, cyclic prefix (CP) and robustness to carrier frequency offset (CFO). In spite of these advantages, many researchers have claimed pros and cons for the usage of FBMC, among those the excessive computational complexity is considered as a major hurdle to deploy for direct employment. We analyze the bit error rate (BER) performance through computer simulation to verify the validity of the proposed method.**

Keywords*— *OQAM-FBMC; WOLA; 5G Waveform; Root raised cosine filter; Prototype filter

I. INTRODUCTION

The offset quadrature amplitude modulation (OQAM)-filter bank based multicarrier (FBMC) is one of the candidates as new waveforms in 5G communications [1, 2] since it provisions a promising capability of reliable spectrum sharing for the secure coexistence according to its inherent high degree of frequency selectivity. Regardless of considerable advantages, so far the usage of OQAM-FBMC has been precluded for the deployment because of its considerable amount of computational complexity. On the purpose of the reduction in computational complexity, various modified versions of OQAM-FBMC transceiver structure have been introduced [3, 4]. In the field of multirate signal processing, [5] recall the windowed overlap-add method considered as an alternative approach widely utilized in multicarrier communication systems such as the discrete multitone (DMT) modulation or the orthogonal frequency-division multiplexing (OFDM) [6]

This paper introduces a novel structure for implementing OQAM-FBMC transmitter and receiver based on the WOLA approach with quantifying computational complexity via taking account of the total number of the complex multipliers used having a form of the function steered by the size of the window and the number of subbands.

Section II deals with the theoretical backgrounds related to the realization of the WOLA-based OQAM-FBMC transceiver imposing the efficient ways of waveform generation and reception in the aspect of computational complexity. Section III provides the simulation results assessing the performance of the modified OQAM-FBMC structure with verifying the consistency of BER

II. PROPOSED WOLA BASED OQAM-FBMC TRANSCEIVER

Significant preponderant capability on the usage of WOLA originates on the flexibility of determining the number of subbands M and decimation factor K. Precisely, according to many related works, the WOLA does not necessitate any restriction on the relationship between M and K, whereas the PPFB does. This positive characteristic enables to adjust the ratio between M and K freely. Thus, this degree of freedom can invoke an opportunity of more efficient use of spectrum without the expense of transmission bandwidth subject to agreeing on the interference constraints for given overlapping factor Q. Without the loss of generality, assuming $M = 2K$, the following subsections deal with the theoretical background of the proposed WOLA structures applying for the realization of OQAM-FBMC transceiver with imposing relevant positive features.

A. Proposed WOLA based OQAM-FBMC Transmitter

Referring Fig. 1, on the usage of the causal PF filter, it can express the m-th subband OQAM encoded waveform as the following ;

$$u_m(k) = \sum_{l=-\infty}^{\infty} h_{PF}(k - lK)\,\hat{x}_m(l) W_M^{m \cdot k} \tag{1}$$

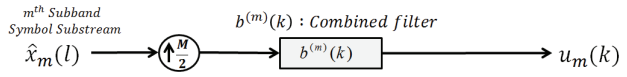

Fig. 1. Structure for generating m-th subband OQAM coded signal.

Subsequently, the overall OQAM-FBMC waveform to be transmitted can be represented by

$$u(k) = \frac{1}{M} \sum_{m=0}^{M-1} u_m(k) = \sum_{l=-\infty}^{\infty} h_{PF}(k - lK) \frac{1}{M} \sum_{m=0}^{M-1} \hat{x}_m(l) W_M^{m \cdot k} \tag{2}$$

Considering the length of causal PF, i.e., $L = QM = 2KQ$, the multiplexed m-th subband symbol sequence $\hat{x}_m(l)$ is confined and nontrivial only for $l = 0,1,2,\cdots,N_S - 1$. The overall OQAM-FBMC waveform $u(k)$ can be rewritten in the form of block-wise representation via replacing the variable k with $r + \alpha K$

in (2) where $r = 0,1,2,\cdots,K-1$ and α=0,1,2,$\cdots, N_S + 2Q - 2$. Furthermore, after replacement, it can describe the $\alpha - th$ block of the OQAM-FBMC waveform of size K expressed as the following ;

$$u(r+\alpha K) \triangleq \sum_{l=0}^{2Q-1} h_{PF}\left(r+(\alpha-l)K\right)\left[\frac{1}{M}\sum_{m=0}^{M-1}\left\{\hat{x}_m(l)W_M^{m\cdot\alpha K}\right\}W_M^{m\cdot r}\right] \quad (3)$$

In the way of processing the inside of bracket in (3), it can adopt the simple $M - pt$ IFFT operation, so that the resulting value denoted by $X_l^{(\alpha)}(r)$ concisely turns out to be

$$\begin{aligned} X_l^{(\alpha)}(r) &\triangleq \frac{1}{M}\sum_{m=0}^{M-1}\left\{\hat{x}_m(l)W_M^{m\cdot\alpha\cdot K}\right\}W_M^{m\cdot r} \\ &= \frac{1}{2}\left\{X_l^e(r)+(-1)^{\alpha}W_M^r\,X_l^o(r)\right\} \end{aligned} \quad (4)$$

Precisely speaking, in RHS of (4), $X_l^e(r) \triangleq 1/K\sum_{\rho=0}^{K-1}\hat{x}_{2\rho}(l)W_K^{\rho r}$ and $X_l^o(r) \triangleq 1/K\sum_{\rho=0}^{K-1}\hat{x}_{2\rho+1}(l)W_K^{\rho r}$ can be achieved by performing $K - pt$ IFFT operations separately on either the even- or the odd-indexed OQAM encoded subband sequences, respectively. Accordingly, $K - pt$ IFFT operations can be accomplished in parallel as shown in Fig. 2. Furthermore, for processing the odd-index OQAM encoded subband sequences, additional weighting operation should be accomplished right after IFFT operation by multiplying $(-1)^{\alpha}W_M^k$, $k = 1,3,5,\cdots,M-1$. In Fig. 2, after the completion of the $K - pt$ IFFT operations for each time instance l, corresponding results are set aside in a series of block memories to make use of them repeatedly until the completion of the achievement of all the vectors $\left\{\mathbf{X}_l^{(\alpha)}\right\}_{\alpha=0}^{N_S+2Q-2}$. Here, it is worthwhile to mention that the weighting function $(-1)^{\alpha}W_M^k$ associated with the block index α appears only for the odd-numbered subband index k. Thus, the above block-wise operation provisions some insight intuitively, so that it can achieve the chance of reducing the computational complexity. With considering (4), it can draw the $\alpha - th$ block of the overall synthesized OQAM-FBMC waveform described by

$$u(r+\alpha K) = \sum_{l=0}^{2Q-1} h_{PF}\left(r+(\alpha-l)K\right)\cdot X_l^{(\alpha)}(r) \quad (5)$$

Specifically, (5) reflects the overall OQAM-FBMC waveform achieved via carrying out a series of a block-wise procedure consisting of a series of shifting & windowing operations. Here, after the construction of temporally aligned $N_S + 2Q - 1$ blocks, the windowing operation carries out by multiplying a series of concatenated blocks, namely the temporally shifted IR of PF of length L, in which each block consists of the length-K outputs.

To represent the above shifting & windowing operation in mathematical derivations, define the $\alpha - th$ block of the overall OQAM-FBMC waveform as $\mathbf{u}^{(\alpha)}$, then we can represent the resulted waveform in the form of the summation of block-wise multiplications as the following ;

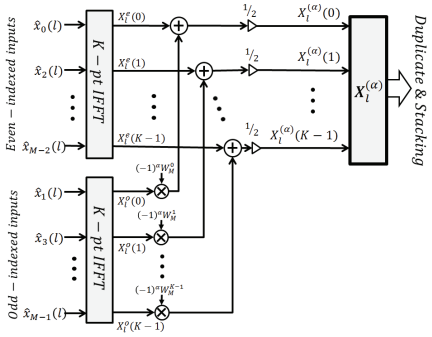

Fig. 2. Reduced operation structure of M − pt IFFT transformations.

$$\mathbf{u}^{(\alpha)} = \sum_{l=0}^{\alpha}\mathbf{X}_l^{(\alpha)} \circ \mathbf{h}_{PF}^{(\alpha-l)} \quad (6)$$

where $\mathbf{u}^{(\alpha)} = \left[u(\alpha K) \quad u(1+\alpha K) \quad \cdots \quad u(K-1+\alpha K)\right]^T$,

$\mathbf{h}_{PF}^{(\alpha)} = \left[h_{PF}(\alpha K) \quad h_{PF}(1+\alpha K) \quad \cdots \quad h_{PF}(K-1+\alpha K)\right]^T$,

$\mathbf{X}_l^{(\alpha)} = \left[X_l^{(\alpha)}(0) \quad X_l^{(\alpha)}(1) \quad \cdots \quad X_l^{(\alpha)}(K-1)\right]^T$.

In (6), ° is the Hadamard product operator indicating block-wise windowing process in between the block of $\mathbf{x}_l^{(\alpha)}$ and that of PF $\mathbf{h}_{PF}^{(\alpha)}$, and the $r - th$ element of $\mathbf{x}_l^{(\alpha)}$ can be expressed by

$$X_l^{(\alpha)}(r) = \frac{1}{2}\left\{X_l^e(r)+(-1)^{\alpha}W_M^r X_l^o(r)\right\} \quad (7)$$

With regarding (6) and (7), the further derivations and modifications give rise to Fig. 10 by which it can visualize the above shifting & windowing process and how to generate the overall OQAM-FBMC waveform $u(k)$ systematically. Apparently, Fig. 3 represents the whole block-wise process consisting of the shifting & windowing followed by the overlapping. Consequently, at the completion of N_S concatenated block-wise procedures, it can generate the overall OQAM-FBMC waveform $u(k)$ of length $(N_S + 2Q - 1)K$ to be transmitted as a result.

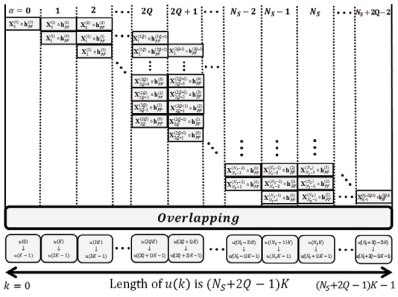

Fig. 3. Shifting and windowing process to generate waveform.

With referring Fig. 3, on the purpose of the exploitation more about the WOLA operation, we release the detailed mathematical derivations afterward. As shown in (7), it can be easy to observe that the block index α can be treated as an indicator to determine if whether or not alter the sign implicitly. According to

the value α which is even or odd, the elements residing both in the $r-th$ position of $\mathbf{x}_l^{(e)}$ and $\mathbf{x}_l^{(o)}$ are equivalent to $\left(X_l^e(r)+W_M^r X_l^o(r)\right)/2$ and $\left(X_l^e(r)-W_M^r X_l^o(r)\right)/2$, respectively, indicative of (7). More interestingly, presumed that N_s is even, a series of row vectors $\mathbf{x}_l^{(\alpha)}$ can be commonly distinguished by $\mathbf{x}_l^{(e)}$ and $\mathbf{x}_l^{(o)}$ representatively as shown in (8). Here, it is manifest that both of $\mathbf{x}_l^{(e)}$ and $\mathbf{x}_l^{(o)}$ are nothing to do with the block index α.

$$\mathbf{X}_l^{(e)} \triangleq \mathbf{X}_l^{(0)} = \mathbf{X}_l^{(2)} = \cdots = \mathbf{X}_l^{(N_S-2)} \quad \text{and} \qquad (8)$$
$$\mathbf{X}_l^{(o)} \triangleq \mathbf{X}_l^{(1)} = \mathbf{X}_l^{(3)} = \cdots = \mathbf{X}_l^{(N_S-1)}$$

B. Proposed WOLA based OQAM-FBMC Receiver

For taking a step forward via exploiting the structure for OQAM-FBMC receiver based on the proposed WOLA, this subsection begins with reviewing two types of conventional receiver discriminated as in Fig. 4 and Fig. 5. The difference between two types of receivers originates from the location of the delay operator Z whether if the subband index m is even or odd. In Fig. 4 and Fig. 5, '*REAL*' and '*IMAG*' indicate the operators to extract real and imaginary part separately from complex input sample so that the corresponding outputs become real. Moreover, it can apply the angle $\theta_{m,n}=\left(\lfloor m/2 \rfloor + n\right)\pi$ in the form of $e^{j\theta_{m,n}}$ or $je^{j\theta_{m,n}}$ as weighting factors to make real-valued input samples into pure-real or pure-imaginary in an interlaced order by which it can recover OQAM encoded symbol sequence $\hat{x}_m(n)$.

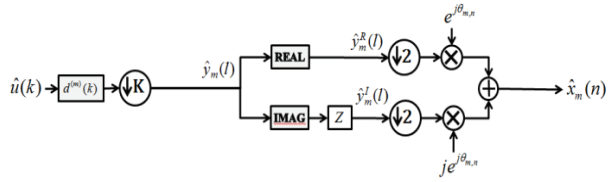

Fig. 4 The structure for recovering OQAM symbol sequence delivered over even-indexed subband.

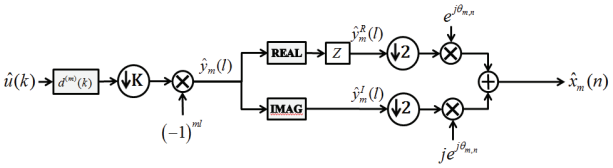

Fig. 5 The structure for recovering OQAM symbol sequence delivered over odd-indexed subband.

Moreover, in Fig. 4 and Fig. 5, the complex-valued $\hat{y}_m(l)$, is the $m-th$ subband signal resulted from passing $\hat{u}(k)$ through the CBF $d^{(m)}(k)$ followed by weighting $(-1)^{ml}$ subsequently. Therefore, after downsampling chosen as K,

$$\hat{y}_m(l)=(-1)^{ml}\left\{\sum_{k=-\infty}^{\infty} d^{(m)}(lK-k)\hat{u}(k)\right\} \qquad (9)$$

III. PERFORMANCE ANALYSIS AND SIMULATION RESULTS

This section confirms the performance of the proposed WOLA based OQAM-FBMC transceiver in the sense of BER performance. As shown in Fig. 6, it can notice that both theoretical results and WOLA based OQAM-FBMC show the same performance.

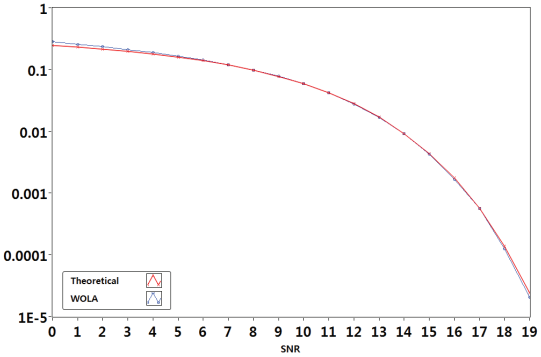

Fig. 6. BER Performance for WOLA based OQAM-FBMC

IV. CONCLUSION

This paper proposed the WOLA-based structure for OQAM-FBMC transceiver, which is employing both simple windowing and overlapping process, relevant simulation results confirmed this affirmative feature with sustaining BER performance.

ACKNOWLEDGMENT

This research was supported by Basic Science Research Program through the National Research Foundation of Korea(NRF) funded by the Ministry of Education(NRF-2016R1D1A1B01007836).

REFERENCES

[1] R. Nissel, S. Schwarz, and M. Rupp, "Filter bank multicarrier modulation schemes for future mobile communications," IEEE Journal on Selected Areas in Communications, vol. 35, issue 8, pp. 1768-1782, 2017

[2] G. Wunder, P. Jung, M. Kasparick, T. Wild, F. Schaich, Y. Chen, S. Brink, I. Gaspar, N. Michailow, A. Festag, L. Mendes, N. Cassiau, D. Ktenas, M. Dryjanski, S. Pietrzyk, B. Eged, P. Vago, and F. Wiedmann, "5GNOW: Non-orthogonal, asynchronous waveforms for future mobile applications," IEEE Communications Magazine, vol. 52, no. 2, pp. 97–105, February 2014.

[3] IEEE, "IEEE standard for radio interface for white space dynamic spectrum access radio systems supporting fixed and mobile operation," IEEE Std 1900.7-2015, pp. 1-67, 2016.

[4] M. Bellanger, D. Le Ruyet, D. Roviras, M. Terr´e, J. Nossek, L. Baltar, Q. Bai, D. Waldhauser, M. Renfors, T. Ihalainen et al., "FBMC physical layer: a primer," PHYDYAS, January, 2010.

[5] R. E. Crochier, "A weighted overlap-add method of Fourier analysis/synthesis," IEEE Trans. Acoust. Speech Signal Process., vol. 28, no. 1, pp. 99-102, Feb. 1980.

[6] Y. Lin, S. Poong, and P. P. Vaidyanathan, Filter bank transceivers for OFDM and DMT systems, Cambridge University Press, 2011.